Extended analysis on Line-Line and Line-Ground faults in PV arrays and a compatibility study on latest NEC protection standards

Pillai , Dhanup S.; Ram, J. Prasanth; Rajasekar, N.; Mahmud, Apel; Yang, Yongheng; Blaabjerg, Frede

Published in:
Energy Conversion and Management

DOI (link to publication from Publisher):
10.1016/j.enconman.2019.06.042

Publication date:
2019

Document Version
Accepted author manuscript, peer reviewed version

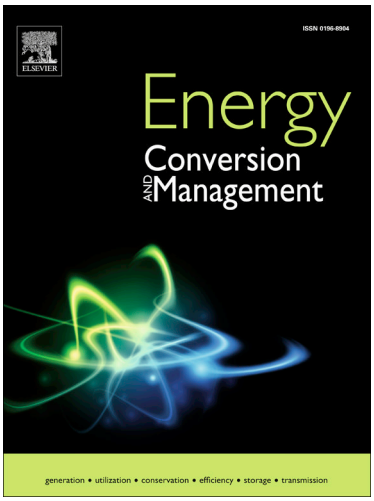

Extended Analysis on Line-Line and Line-Ground Faults in PV Arrays and a Compatibility Study on Latest NEC Protection Standards

Dhanup S. Pillai, J. Prasanth Ram, N. Rajasekar, Apel Mahmud, Yongheng Yang, Frede Blaabjerg

PII: S0196-8904(19)30713-7
DOI: https://doi.org/10.1016/j.enconman.2019.06.042
Reference: ECM 11731

To appear in: *Energy Conversion and Management*

Received Date: 1 February 2019
Revised Date: 25 March 2019
Accepted Date: 18 April 2019

Please cite this article as: D.S. Pillai, J. Prasanth Ram, N. Rajasekar, A. Mahmud, Y. Yang, F. Blaabjerg, Extended Analysis on Line-Line and Line-Ground Faults in PV Arrays and a Compatibility Study on Latest NEC Protection Standards, *Energy Conversion and Management* (2019), doi: https://doi.org/10.1016/j.enconman.2019.06.042

Extended Analysis on Line-Line and Line-Ground Faults in PV Arrays and a Compatibility Study on Latest NEC Protection Standards

Name of authors:	[2]Dhanup S. Pillai, [1]J Prasanth Ram, [2]N. Rajasekar, [3]Apel Mahmud, [4]Yongheng Yang and [4]Frede Blaabjerg.
eMail id:	dhanup.research@gmail.com , jkprasanthram@gmail.com natarajanrajasekar@gmail.com, apel.mahmud@deakin.edu.au, yoy@et.aau.dk and fbl@et.aau.dk
Affiliation:	[1]Department of Electrical and Electronics Engineering, KPR Institute of Engineering and Technology, Arasur, Coimbatore, Tamil Nadu, India. [2]Solar Energy Research Cell, School of Electrical Engineering, Vellore Institute of Technology, Vellore, India. [3]School of Engineering, Faculty of Science Engineering & Built Environment, Deakin University, Geelong Waurn Ponds Campus, Locked Bag 20000, Geelong, VIC 3220 [4] Department of Energy Technology, Aalborg University, Aalborg DK-9220, Denmark .

Corresponding author:

N. Rajasekar,
Professor,
Solar Energy Research Cell,
School of Electrical Engineering,
VIT University, Vellore, Tamil Nadu
India - 632014.
Email: natarajanrajasekar@gmail.com
Contact Number: +91 9952362301.

ABSTRACT: Even with the expeditious progress in global Photovoltaic (PV) power generation, faults occurring in PV systems pose excessive challenges to the productivity and reliability of PV installations. Though specific installation standards have been developed for the protection of PV systems, the compatibility of these standards to cope with the unique operating characteristics of PV generating systems is questionable and hence, needs critical evaluation. Therefore, this paper briefly analyzes the standards available for the protection of PV systems, investigates the protection challenges and inspects the compatibility of latest National Electric Code (NEC) standards to protect PV arrays against Line-Line (LL) and Line-Ground (LG) fault occurrences. In particular, this article conducts a detailed behavioral study on LL and LG faults and evaluates the compatibility of NEC standards in the context of: 1) Varying mismatch levels, 2) Impact of Maximum Power Point Trackers (MPPTs) and 3) Changing irradiation levels. Detailed simulations as well as experimental analysis have been carried out to clearly portray the challenges in LL/LG fault detection despite by following new NEC recommendations. Further, based on the implications attained, some suggestions for reliable fault detection have also been presented that are expected to enhance the reliability of LL/LG fault detection in PV systems.

Keywords: Fault detection, Line-Line Faults, Line-Ground Faults, PV systems, NEC, Protection Standards

Acronyms

AFCI	Arc Fault Circuit Interrupter	MPPT	Maximum Power Point Tracker
AFD	Arc Fault Detector	NEC	National Electric Code
CCC	Current Carrying Conductor	OC	Open Circuit
EGC	Equipment Grounding Conductor	OCPD	Over Current Protection Device
GFDI	Ground Fault Detection and Interruption	PS	Partial Shading
IMD	Insulation Measurement device	PV	Photovoltaic
LG	Line-Ground	RCD	Residual Current Detector
LL	Line-Line	SC	Short Circuit

Symbols

I_a	Array current	I_{mp}	Current at maximum power point
$I_{a\ post\ fault}$	Post fault array current	I_{SC}	Short circuit current
$I_{a\ pre\ fault}$	Pre fault array current	V_{mp}	Voltage at maximum power point
I_f	Fault or GFDI current	V_m	Mismatch voltage
$I_{f\max}$	Maximum fault or GFDI current	V_{OC}	Open circuit voltage
I_{fs}	Faulty string or OCPD current	n	Number of PV strings

$I_{fs\max}$	Maximum faulty string or OCPD current	Z_m	Mismatch Impedance

1. Introduction

In modern era, electric power generation from photovoltaic resources has conceived a huge market in micro grid environment. On the other hand, despite all benefits and research advancements that have been made so far, photovoltaic (PV) systems are highly vulnerable to fault occurrences that drastically reduce the efficiency and safety [1]. For instance, undetected faults in PV systems recently provoked severe fire hazards in California and Bakersfield [2]. Nevertheless, faults in PV systems and the necessity of advanced protection standards are less addressed and investigated. Thus, fault analysis in solar PV arrays becomes a fundamental requirement to increase the reliability of PV systems.

Very few standards are developed and recommended for protection in PV systems against faults and electric shocks; at international level, IEC 60364-7-712 [3], IEC 62548 [4] and IEEE standard 1374 [5], at national level, NEC (National Electrical Code) article 690 [6] and Spanish Royal Decree 1663 [7]. Meanwhile, protection standards such as IEC 61140 [8] and IEC 60364-41 [9] that are suitable for conventional power systems are not compatible with PV systems since PV systems are relatively new and posses unique operating characteristics that are no way comparable to conventional power generating units [10-12].

NEC article 690 covers numerous aspects of PV protection and is widely practiced around the globe. Unfortunately, NEC 690 also lacks features that address important practical issues related to PV system safety [1, 14]. In this regard, limitations of NEC 1998 and 2008 standards in Line-Ground (LG) fault detection are studied in [15, 16], Line-Line (LL) fault detection challenges involved with NEC 2011 are investigated in [17] and the adverse effect of Maximum Power Pointing Trackers (MPPTs) towards LL fault detection is discussed in [18]. It is important to note that, the experimentations carried out in aforesaid works [15, 16 and 18] were too short, and the analysis was restricted to standard PV operating conditions only. While in [17], the compatibility of NEC standards has been evaluated for various PV operating conditions with different fault impedances. However, as for the earlier works, the findings were not generalized since the study was constrained to a single PV system configuration. Also, the objective of all aforementioned works was only to showcase LL/LG fault detection challenges without providing any suggestions for improvement. It is important to note that, though researches available till date in literature attempts to analyze the incompatibility of NEC standards, conclusive results with respect to various practical operating conditions of PV systems are yet to be arrived. Moreover, regardless of these short

investigations, even the latest NEC 2017 standards are not revised to counter act the protection challenges involved.

On this note, the proposed work endeavors to provide much detailed investigations to understand the unique behavior of LL and LG faults in PV arrays. Furthermore, new mathematical equations based on the equivalent circuit of a faulty PV array are derived to determine the fault current levels; that enhances PV array fault analysis possibilities. In addition, in order to set accurate benchmarks, extensive fault analysis in various unique PV operating conditions is performed and the compatibility of latest NEC 2017 protection standards for LL/LG detection is evaluated. Moreover, to generalize the findings attained with respect to fault current magnitudes, the proposed study is extended to two different PV configurations. Further, based on the critical implications attained from the analysis, some suggestions to achieve reliable LL/LG fault detection are also presented. On the whole, to be versatile from the existing scientific contributions, this research attempts to: 1) Provide a brief overview on various fault occurrences in PV systems, 2) Perform a detailed behavioral analysis on LL and LG faults in PV arrays, 3) Analyze the effectiveness of latest NEC standards for LL/LG fault detection with respect to: a) PV array size, b) Variation in fault mismatch levels, c) Application to MPPT and non-MPPT based PV systems and d) Adaptability in varying irradiation levels, and 4) Suggest some valuable facts that are expected to be meritorious to accomplish dependable LL/LG fault detection for PV arrays.

2. Typical PV Faults and NEC Protection Standards

2.1 Faults in PV Arrays

PV arrays are frequently challenged by two common fault scenarios: (1) Electrical faults and (2) Shade faults. Electrical faults occur due to abnormalities that arise in the internal electrical configuration of the system; while, shade faults are induced by change in insolation levels and the external environment. Further, both these faults are bound to have significant impact on the output characteristics of any standalone and grid connected PV system. Typical PV fault scenarios are depicted in Fig.1.

2.1.1 Electrical Faults

Generally, electrical faults can be: 1) Line-Ground (L-G), 2) Line-Line (LL), 3) Open Circuit (OC) and 4) Arc faults. Among which LG fault commonly occur due to accidental connection between Earth Ground Conductor (EGC) and Current Carrying Conductor (CCC); either caused by internal PV cell failure or insulation failure of cables [14]. On the other hand, LL faults are created by accidental short circuit between any two points in the PV

array. Further, LL fault in the same string and two different strings are referred as intra string and cross string faults respectively. Any open circuit between two panels induces open circuit faults and interrupts the current flow [1]. Usually, OC faults are after effects of short circuit faults or connection failures in the PV array. While, arc faults that cause severe fire hazards are either of series or parallel type and are created by open circuit faults in a string or due to insulation breakdown between two pints of adjacent strings [14]. In addition, any improper switching of MPPT controller and age factor increases the thermal stress on the switch that leads to converter faults [19]. In addition to above, abnormal charging conditions or internal cell damage create battery bank faults. Even though battery bank faults do not affect the PV array, it adversely affects energy management systems. Besides these faults, abnormalities in inverter units and utility grid can also affect the non-islanding operation of PV systems [20].

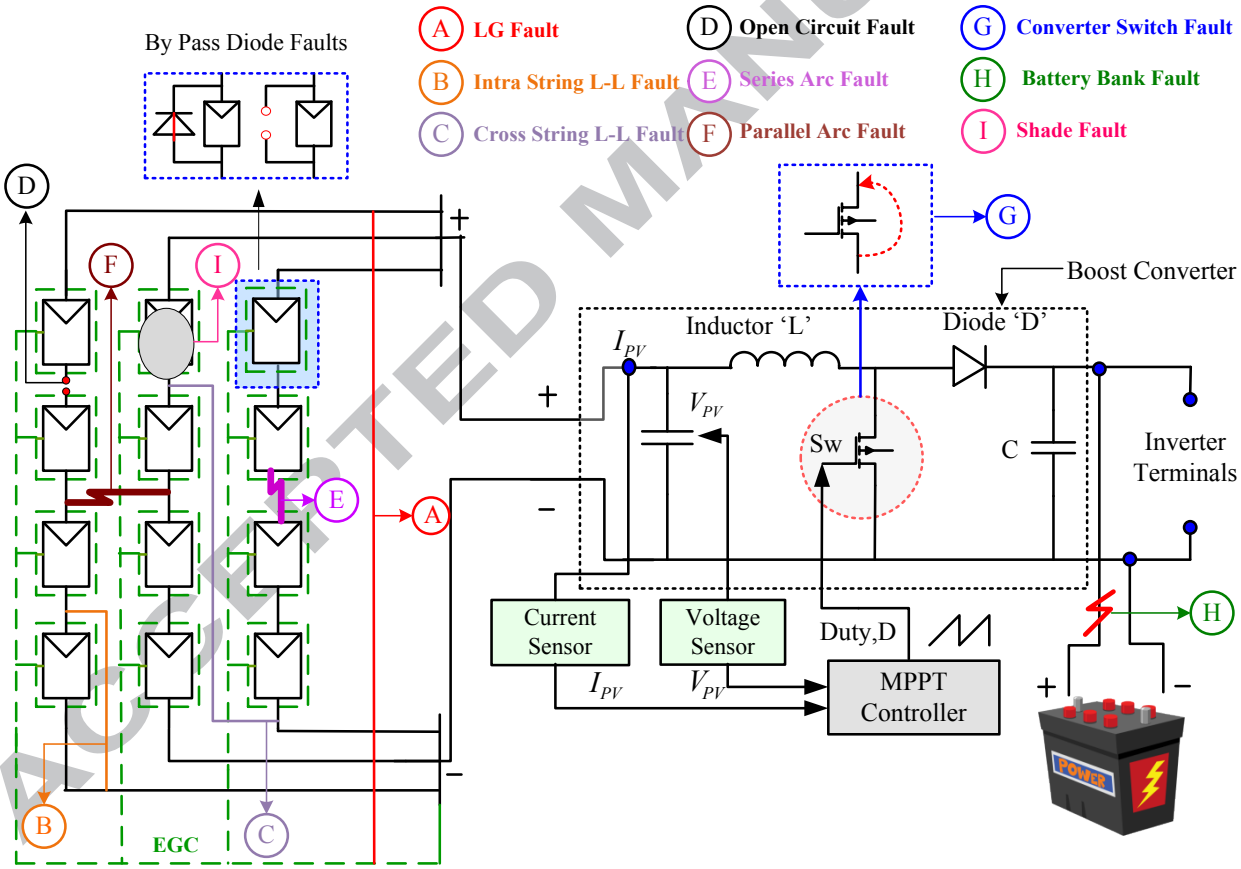

Fig.1. Various faults occurring in a PV system

2.1.2 Shade Faults

Unlike electrical faults, shade faults are created by the uneven distribution of shades over the PV array. Partial Shading (PS) occurs due to any one of the following events [21, 22]: 1) Building shadows, 2) Tree shadows, 3) Passage of clouds, 4) Bird droppings and 5) Dust accumulation on the panel surface. In most cases, partial shading is temporary in nature. However, shade due to dust accumulation and bird droppings is permanent that require

immediate intervention. Even though array reconfiguration techniques [23] to certain extend reduce the impact of shade faults and enhances the power output; mismatch effect still persists that can lead to the formation of hot spots and degradation of PV panels. Hence, detecting permanent and prolonged PS in PV systems must be given due importance.

2.2 NEC Protection Standards

Fault occurrence in a PV system drastically reduces the power output and any undetected fault accelerates the degradation of PV panels. Further, it is difficult to distinguish the faults from normal operating conditions by traditional protection schemes since; the change in the current levels might not be substantial. Moreover, the magnitude of fault current levels in PV systems is highly dependent on the instantaneous irradiation levels, PV array size and the location of the fault. Therefore, defining accurate protection standards becomes crucial to avail timely detection of faults in PV systems. In this regard, article 690 in NEC specifically deals with the practices to be followed while installing PV systems and it also covers all general standards that are applicable to PV installations. Table 1 specifies the NEC standards amended for various protection aspects of PV installations.

2.2.1 Protection Standards Specified in Article 690

NEC article 690 specifically details the protection standards to be followed against three fault occurrences: 1) Short circuit, 2) Ground and 3) Arc faults. For reliable protection against short circuits, it recommends Over Current Protection Device (OCPD) for faulty string isolations whenever the line current exceeds 156% of the rated Short Circuit (SC) current of the string. Similarly, to avail ground fault protection: 1) PV systems must be grounded using EGC (Copper or Aluminium) and the point of grounding must be the negative terminal of the PV array and 2) Ground Fault Detection and Interruption (GFDI) fuses must be installed for each PV array in the system. The standards recommended for the selection of EGC and GFDI fuses are listed in Table 2 and Table 3 respectively. An alternative protection scheme for ungrounded systems is the use of Residual Current Detector (RCD) to measure the residual current between the positive and the negative terminal of the PV array. When the residual current exceeds the threshold limit, RCDs trip the circuit and isolates the PV array. For arc fault protection in PV systems, NEC 690 recommends the use of Arc Fault Circuit Interrupter (AFCI) and Arc Fault Detector (AFD). AFCIs are commercially available as an integrated device in solar inverters; distinctively, AFDs are only detection devices installed in each PV string. The standards recommended for these devices are presented in Table 4. The connection diagrams of all the protection devices are illustrated

in Fig. 2(a) to Fig. 2(e). Apart from the live protection devices discussed, Insulation Measurement Device (IMD) is also used as an off line measurement tool that can effectively check for insulation failures in the CCC; thereby capable of detecting ground faults and OC faults. A detailed techno commercial analysis of all the protection devices recommended by NEC article 690 is illustrated in Table 5. It is important to note that even though commercial AFCIs are available up to 400A rating, the product safety standard UL 1699B for DC arc fault protection presently covers products rated up to 40A only. Hence, NEC 2017 article 690.11 exempts large PV installations from installing arc fault protection devices.

Table 1
Standards applicable for protection of PV systems in NEC

Sl. No	Article	Standards Specified
1	110	General Requirements for all Low Voltage (LV), Medium Voltage (MV) and High Voltage (HV) electrical installations
2	250	Grounding standards required for all electrical installations
3	300	Different wiring standards to be practiced for LV, MV and HV electrical Installations
4	310	Standards recommended for selecting wiring conductors
5	480	Requirements for a battery storage system
6	690	Protection standards that are to be specifically practiced for PV installations

Table 2
Sizing standards for Grounding Conductors

Sl. No	Rating of trip device	Size of the grounding conductor in SWG	
		Copper	Aluminum
1	15 A	14	12
2	20 A	12	10
3	60 A	10	8
4	100 A	8	6
5	200 A	6	4
6	300 A	4	2
7	400 A	3	1
8	500 A	2	1/0
9	600 A	1	2/0

Table 3
Standards for GFDI Fuse selection

DC rating of the inverter	GFDI fuse rating to be selected
0-25 KW	1 A
25-50 KW	2 A
50 -100 KW	3 A
100- 250 KW	4 A
> 250 KW	5 A

Table 4
Arc Trip Standards

Arc Current (A)	Arc Voltage (V)	Arc Power (W)	Clearing time	Gap between electrodes
7	43	300	2 seconds	1.6 mm
7	71	500	1.5 seconds	4.8 mm
14	46	650	1.2 seconds	3.2 mm
14	64	900	0.8 seconds	6.4 mm

Table 5
Techno-commercial analysis of standard protection devices

Sl. No.	Protection Device	Ratings Available		Effective Protection Target	Connection	Cost Range
		Current	Voltage			
1	GFDI	1A-5A	150V DC-600V DC	Ground faults in functionally grounded PV systems	Between negative terminal of the array and the ground connector	300-470$
2	OCPD	4A-630A	600V DC -1500V DC	Over current faults in an individual PV string	In line with the string current carrying conductor	15-100$
3	RCD	50A-100A, 100mA-300mA	150V DC-600V DC	Ground faults in floating PV systems	Between positive terminal and negative terminal of the string	190-377$
4	IMD	20mA-200mA	50V DC-1500V DC	Ground faults in the PV array and insulation failures in the current carrying conductors	Varies with measurement	800-1300$
5	AFCI	up to 40A	up to 1000V DC	Series arc faults in PV array	In line with positive terminal in the combiner box	1000-1600$
6	AFD	up to 40A	up to 1000V DC	Series arc faults in PV array	In line with string current carrying conductor	130-200$

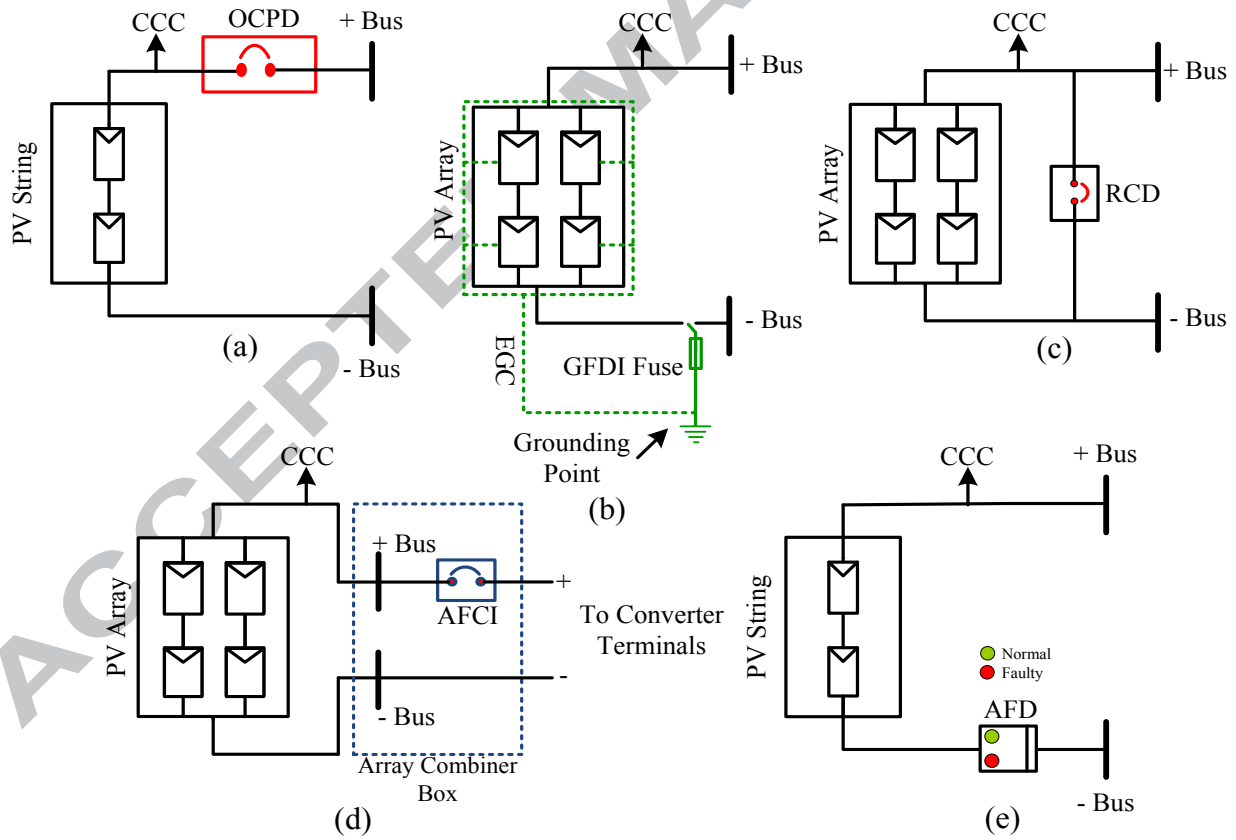

Fig.2. Connection diagrams for various protection devices: (a) OCPD, (b) GFDI Fuse, (c) RCD, (d) AFCI and (e) AFD.

2.3 NEC 2017 updates to article 690

Standards defined prior to 2017 had practical issues and remained unsolved. Hence, NEC code of standards is frequently updated; of which, the latest standards to be followed are NEC 2017. The basic standards for over current protection, ground fault protection and arc fault protection still remains to be the same in NEC 2017. However, some conceptual clarifications and few major updates were newly added. Table 6 details the key updates in NEC 2017. Since isolation of either the positive or the negative conductor is sufficient to isolate the faulty string, the revised 690.9 (C) article recommends the use of only one OCPD per string. Further, as indicated in Table 5, article 690.11 exempts large PV installations from installing arc fault protection devices. The major updates, 690.12 and 690.13 added in NEC 2017 is the inclusion of disconnect standards for PV systems. These standards are specifically intended for safety during emergency conditions and to protect users from electric shocks. Conceptual modification to ground fault protection as per 690.41(B) and 690.42 clarifies that all PV systems are functionally grounded and hence, GFDI fuses must be installed. Note that the overcurrent protection standards amended in NEC are to be practiced for all PV installations having more than two parallel strings.

Table 6
Key updates to Article 690 recommended in NEC 2017

Target	Article	Standards Specified
Over Current Protection	690.9 (C)	Only one over current protection device is required per string and can be installed in either '+' or '-' of the PV array
Arc Fault Protection	690.11	Arc fault protection devices are only available up to a current of 40A and hence, large PV systems are exempted from installing arc fault protection devices
Disconnect Standards	690.12	An emergency trip provision must be provided for avoiding potential electric shocks and fire hazards from PV systems
	690.13	Disconnect devices installed as per 690.12 must be installed at a readily accessible location
Ground Fault Protection	690.41(B), 690.42	Clarifies that all PV installations are functionally grounded and solid groundings are rare and all PV systems must be protected using ground fault protection devices

3. Line-Line and Line-Ground fault Analysis

With the clear understanding on different PV faults and protection standards, it is imperative to provide a general fault behavior analysis with protection devices installed in a PV array. To exemplify the evolution of fault current, LL and LG faults are extensively studied and its impact on the system performance is perceived. For examination, an '$n \times n$' PV array equipped with OCPD and GFDI as shown in Fig. 3(a) is considered and the

evolution of faults is analyzed. Since, the severity of the fault occurrence is determined by the location of the fault point in a PV array, it is mandatory to provide a detailed study on the system behavior with different fault locations as well as with various fault types. Hence, three fault locations indicated in Fig. 3(a) are created and analyzed.

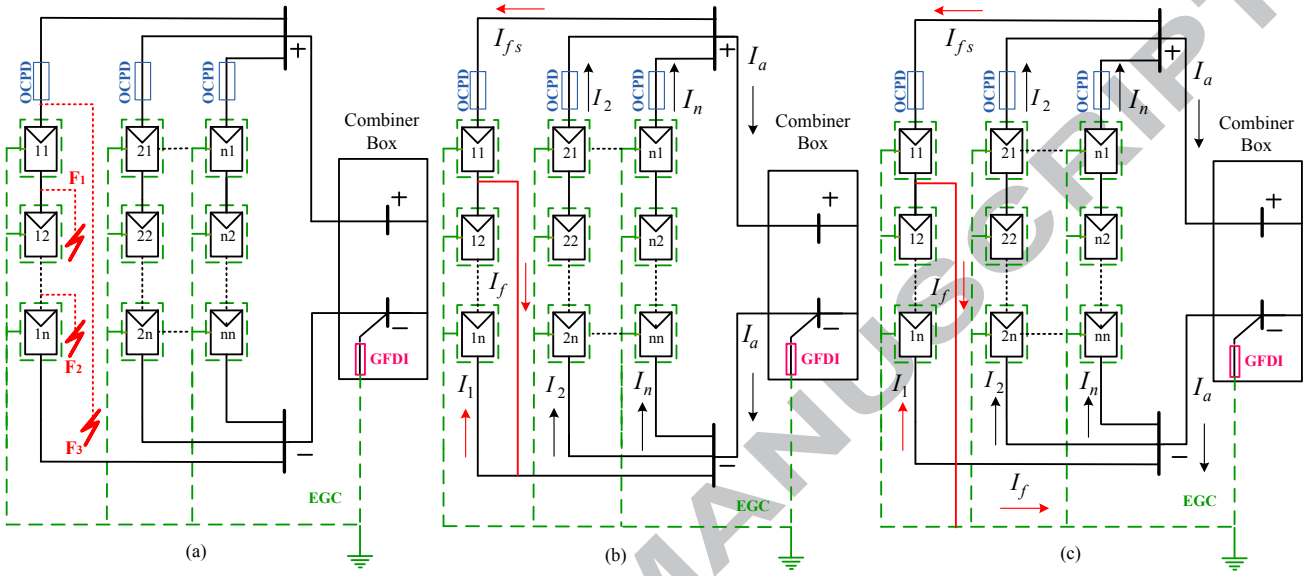

Fig.3. Typical $n \times n$ PV array: (a) Different fault locations, (b) High mismatch intra string LL fault and (c) High mismatch LG fault.

Any LL/LG fault occurrence at fault location F_1 induces a high mismatch of $n-1$ panels between the fault points; while, the lowest mismatch (single module) is created at fault point F_2. Further, fault at point F_3 completely short circuits the PV array. To determine the severity of faults and to quantify the mismatch levels, the term mismatch impedance (Z_m) is introduced that decreases as the mismatch level increases. Further, it can be calculated as the ratio of voltage mismatch (V_m) to the fault current (I_f) at a particular fault location.

$$Z_m = \frac{V_m}{I_f} \quad (1)$$

3.1 Fault evolution in a PV array

In the event of low mismatch impedance LL and LG faults, the faulty string receives a high mismatch of '$n-1$' panels and are characterized by high reverse current flow through the faulty string [1, 14 and 17]. As depicted in Fig. 3(b) and Fig. 3(c), prior to the faults, the PV array delivers an array current of 'I_a' with each string contributing equal currents, '$I_1, I_2, I_3 .... I_n$'. However, due to the occurrence of high mismatch fault ('$n-1$' panels) in the first PV string, the string experiences two non-ideal current flows as indicated in Fig. 3(b): 1)

'I_{fs}' – back fed current flowing in the reverse direction through the OCPD fuse and 2) 'I_f' – the total fault current flowing through the fault path. Further, at the circuit level, it can be understood from Fig. 3(b) and 3(c) that, the sole difference between an LL and LG fault in PV arrays is the non-identical flow of fault currents. It can be clearly visualized from Fig. 3(c) that 'I_f' directly flows through GFDI fuse in the case of an LG fault unlike LL faults. More importantly, during both the fault instances illustrated in Fig. 3(b) and Fig. 3(c) respectively, 'I_1' represented will obviously be the short circuit current of a PV module since the short circuited modules operate the short circuit point in its respective I-V curve yielding zero voltage output.

3.1.1 Identifying faulty string current (OCPD current)

For the faulty PV array shown in Fig. 3(b) and 3(c), the governing equations that correspond to faulty string and fault current can be represented as:

$$I_{fs} = \left| I_a - \left(I_2 + I_3 + \ldots I_n \right) \right| \quad (2)$$

$$I_f = I_{fs} + I_1 \quad (3)$$

However, if the fault occurs in the lower half of the string, the voltage mismatch between the healthy strings and the faulty string will be very low and therefore, it might not be severe enough to cause a reverse current flow [17]. Undoubtedly, for low mismatch faults occurring at location 'F_2' in Fig. 3(a), $I_1 >> I_f$ due to the absence of reverse current. Hence, in such cases, Eq. (3) must be modified as:

$$I_1 = I_{fs} + I_f \quad (4)$$

3.1.2 Identifying fault current (GFDI current)

As 'I_{fs}' is the back fed current flowing through the OCPD fuse, its magnitude can be easily calculated from Eq. (3) and Eq. (4) once the value of 'I_f' is known. This is because, in both equations 'I_1' specifies the SC current of the module/string; which, for Standard Test Conditions (STC) is a data sheet value and for low irradiation conditions is the ratio of instantaneous array current (I_a) to the number of strings (n).

$$I_1 = \frac{I_a}{n} \quad (5)$$

Now, to identify the magnitude of 'I_f', the pre fault and post fault array currents can be efficiently utilized. To comprehend this behavior, it is mandatory to have an enhanced understanding on the overall behavior of a PV array under LL/LG fault conditions. For

which, the equivalent circuit of a normal and faulty PV array are considered as shown in Fig. 4(a) and Fig. 4(b) respectively. As shown in Fig. 4(a), the entire pre fault array current flows to the load terminals in normal working conditions. In sequence, if an LL/LG fault occurs with particular line impedance (generally 0-1Ω), the total array current gets divided into two (see Fig. 4(b)): 1) current flowing to load terminals and 2) current flowing through fault path. Now that PV being a current source, the magnitude of current flowing through the fault path (I_f) will be a fraction of the pre fault array current and is determined by the amount of current PV delivers to the load. The post fault load current depends on the impedance of the load, which decides the operating point (current and voltage co-ordinates) in the I-V curve and subsequently, the remaining current flows through the fault path. Now, if '$I_{a\ pre\ fault}$' is the normal pre fault array current and '$I_{a\ post\ fault}$' is the post fault array current at load terminals at a particular operating condition, then, mathematical relation for 'I_f' can be generalized as:

$$I_f = I_{a\ pre\ fault} - I_{a\ post\ fault} \quad (6)$$

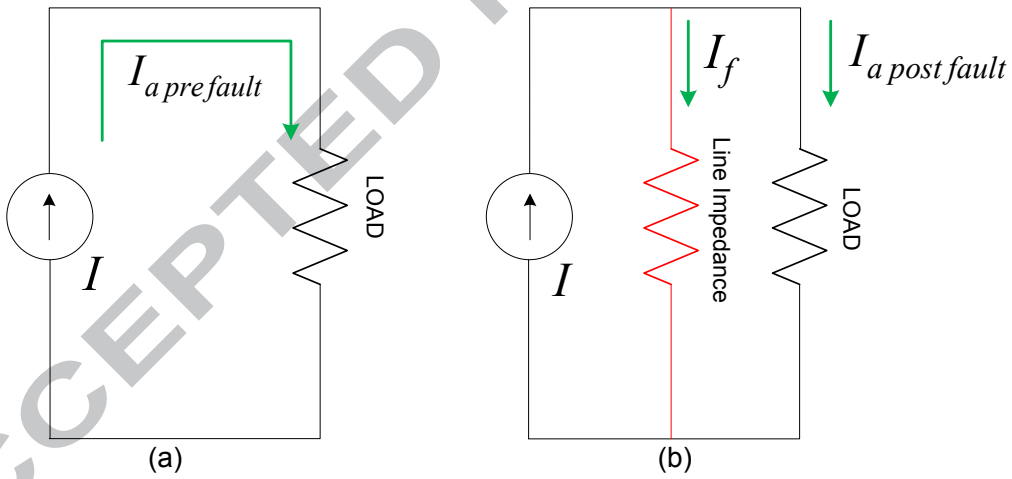

Fig.4. Equivalent circuit of a PV array: (a) Normal, (b) Faulty

3.1.3 Identifying maximum fault current levels

To examine the maximum fault current levels, fault location 'F_3' in the 1st PV string indicated in Fig. 3(a) is considered and analyzed. Since any LL/LG fault at location 'F_3' completely short circuits the PV array, each string operates at its individual short circuit points. At this instant, if '$I_{SC2,}I_{SC3}...I_{SCn}$' are the SC currents of healthy strings, then the maximum reverse current experienced by the faulty string can be expressed as;

$$I_{fs\max} = I_{SC2} + I_{SC3} + ...I_{SCn} = (n-1)I_{SC_{string}} \quad (7)$$

Where 'n' is the total number of strings and '$I_{SC_{string}}$' is the SC current of an individual string. Undoubtedly, '$I_{a\ post\ fault}$' will be zero for this case since, all healthy string are feeding the fault point. Therefore, from (3), the maximum fault current at this instant will be:

$$I_{f\max} = (n-1)I_{SC_{string}} + I_{SC_{strig}} = n \times I_{SC_{string}} \quad (8)$$

3.1.4 Identifying fault current levels from transitional array characteristics

As the pre fault and post fault array currents can be attained from the transitional characteristics of a PV array, the magnitude of fault current (GFDI current) can be calculated using Eq. (3). This is explicitly shown using the experimental result represented in Fig. 5 obtained in response to an LL/LG fault; where '$I_{a\ pre\ fault}$' and '$I_{a\ post\ fault}$' at the load terminals is indicated. As clearly illustrated, the difference between post fault and pre fault array currents gives the value of 'I_f'. Now that the fault current is obtained, Eq. (2) and Eq. (3) can be efficiently utilized to identify the OCPD currents. Note that the value of 'I_1'can be easily determined using Eq. (5) at all operating conditions of the PV array.

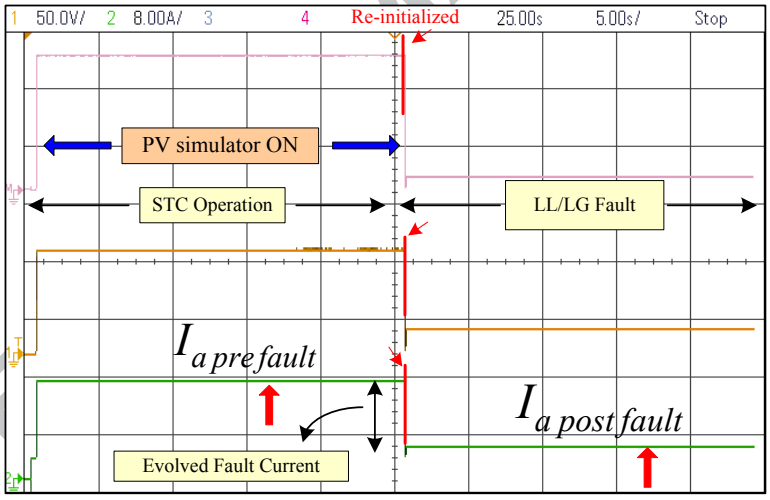

Fig.5. Identification of fault current from transitional array characteristics

4. Suitability analysis on NEC 2017 standards for LL and LG fault detection

The signature of faults on the PV array is unique and the protection challenges primarily rely on three major factors [1, 14 and 17]: 1) Mismatch impedance determined by fault location, 2) Presence of MPPT controller and 3) Instantaneous irradiance falling on the PV array. Hence, any proposed protection standards for PV systems must have the following inherent and inevitable capabilities: a) Irrespective of varying fault impedances, protect the PV system, b) Detect faults even in low irradiation levels and c) Ability to counter act the MPPT effects. Hence, the compatibility of NEC 2017 standards is verified via a detailed

analysis based on four practically relevant operating conditions: 1) Varying mismatch impedance without MPPT at Standard Test Conditions (STC), 2) Varying mismatch impedance with MPPT at Standard Test Conditions (STC), 3) Varying irradiation levels without MPPT and 4) Varying irradiation levels with MPPT. Simulations are performed in MATLAB/SIMULINK with a 5×5 PV array built with solar tech S55 PV modules having following data sheet specifications: V_{OC}=22.1V, V_{mp} =18.18V, I_{SC}=3.45A, I_{mp} =3.31A and P=55W.

4.1 Analysis with varying mismatch impedances

The compatibility of NEC 2017 standards are analyzed with respect to varying mismatch impedances and for each fault case, the suitability is studied with/without MPPT. For precision, fault current, faulty string current and array current are noted for each case along with the device currents. For the system configuration considered, 'I_{SC}' of each individual string is 3.31A. Hence, the recommended minimum rating of the OCPD as per NEC 2017 article 690.9 (B) should be 5.1A (rated for 156% of the SC current of a string) and the trip point as per PV fuse standard UL2579 [1] will be 7 A. Further, for the considered 1.375kW PV system, GFDI fuse selected in accordance with the DC rating of the inverter specified in Table 3 is 1A. Simulations are carried out for four different mismatch impedances corresponding to four different fault locations created in the second PV string: 7Ω, 7.5Ω, 8.5Ω and 11.2Ω respectively. Table 7 elucidates the results obtained for LL/LG fault analysis without MPPT whereas Table 8 illustrates the results for faults simulated with MPPT.

4.1.1 LL Fault analysis without MPPT

When LL faults are created in the absence of MPPT at varying mismatch impedances, the faulty string current varies in the range of -9.38A to 1.3A (case 1-4 in Table 7). The string current values that corresponds to fault impedances 7Ω, 7.5Ω, 8.5Ω and 11.2Ω are -9.38A, -5.5A, -1.85A and 1.3A respectively. Here, the negative sign indicates that the faulty string experiences a back fed current in the opposite direction (cases 1-3). However, when the fault impedance increases to 11.2Ω (case 4), there is no reverse current flow in the faulty string. It is important to note that irrespective of the current direction, OCPD trips when the string current magnitude exceeds its trip point of 7A. Therefore, OCPD trips only for the case of lowest mismatch impedance, 7Ω and remains unconditionally inactive for rest of the cases. Hence, faults that occur with impedances 7.5Ω, 8.5Ω and 11.2Ω will remain undetected in the PV array. Furthermore, if the DC cable rating for this faulty string is selected according to

NEC 690.8 (B), the maximum current that the cable can withstand is 5.1A; which is lower than the undetected LL fault current of 5.5A for the second case with impedance of 7.5Ω. Hence, the recommendation made in NEC to interrelate article 690.8 (B) and 690.9 (B) is unsafe. Overall, the protection standards amended in NEC 2017 are unreliable for the protection of PV systems against LL faults.

4.1.2 LG Fault analysis without MPPT

Like LL faults, LG scenarios are also created at the same fault locations and the results presented in Table 7 (case 5 to case 8). For the protection of PV systems against LG faults, both GFDI and OCPD are involved; since LG faults are also characterized by over currents. From the results presented, it is evident that at low mismatch impedance (7Ω), GFDI and OCPD currents are substantial to trip the devices; while, GFDI alone trip for the remaining cases of 7.5Ω, 8.5Ω and 11.2Ω. Even though the GFDI currents of 5.21A and 1.97A that correspond to fault impedances of 8.5Ω and 11.2Ω is high enough to blow 1A GFDI fuse, this might not be possible for higher rated systems with same number of strings; since, GFDI fuse rating is decided by the DC rating of the inverter. For instance, if the selected GFDI rating is 5A, both LG faults of impedances 8.5Ω and 11.2Ω will not be detected. Moreover, undetected ground faults are more dangerous as it may lead to double line-ground faults that can entirely destroy the entire PV array [14]. On the whole, even though NEC 2017 standards can protect small PV systems from ground fault occurrences, reliable protection is not guaranteed for higher rated PV systems particularly when the mismatch impedance is high.

4.1.3 Impact of MPPT on LL and LG faults

Similar analysis has also been performed for varying fault impedances in the presence of MPPT and the results are elucidated in Table 8. As illustrated, irrespective of the mismatch impedances, MPPT optimizes the operating points of the PV array such that it deceives all the protection devices. Hence, the fault current lies within a very narrow range for different mismatch impedances and considerably affects the detection process. Further, it can be visualized that the fault current magnitudes of both LL and LG faults in all the cases are appreciably reduced to more than 95% of its original value. Subsequently, there is no reverse current flow through the faulty string and the OCPD currents are by far less than the OCPD trip point set to 7A. In addition, the GFDI currents are reduced to 0.66A, 0.75A, 0.82A and 0.83 A respectively from 12.73A, 8.85A, 5.21A and 1.97A for mismatch impedances of 7Ω, 7.5Ω, 8.5Ω and 11.2Ω. Undoubtedly, none of these GFDI currents are substantial to blow even 1A the GFDI fuse. It is also important to note that, the overall array current is improved

in each case and is optimized to vary with in a narrow range between 16.02 A and 15.58A. As a summary, neither OCPD nor GFDI standards set by NEC 2017 are functionally capable to negate with MPPTs and hence, irrespective of the mismatch level, all LL and LG faults will remain undetected in any MPPT based PV system for ever.

Table 7
LL and LG fault analysis for varying mismatch levels without MPPT

Fault Type	Case No.	Mismatch Impedance (Ω)	Fault Current (A)	Faulty string OCPD current (A)	GFDI current (A)	Array Current (A)	OCPD Trip	GFDI Trip	Reliable Fault Detection
LL Fault (Intra string)	1	7	12.73	-9.38	0	3.95	Yes	**No**	Yes
	2	7.5	8.85	-5.5	0	7.75	**No**	**No**	**No**
	3	8.5	5.21	-1.85	0	11.315	**No**	**No**	**No**
	4	11.2	1.97	1.3	0	14.31	**No**	**No**	**No**
LG Fault	5	7	12.73	-9.38	12.73	3.95	Yes	Yes	Yes
	6	7.5	8.85	-5.5	8.85	7.75	**No**	Yes	Yes
	7	8.5	5.21	-1.85	5.21	11.315	**No**	Yes	**No**
	8	11.2	1.97	1.3	1.97	14.31	**No**	Yes	**No**

Table 8
LL and LG fault analysis for varying mismatch levels with MPPT

Fault Type	Case No.	Mismatch Impedance (Ω)	Fault Current (A)	Faulty string OCPD current (A)	GFDI current (A)	Array Current (A)	OCPD Trip	GFDI Trip	Reliable Fault Detection
LL Fault (Intra string)	1	7	0.66	2.68	0	16.02	**No**	**No**	**No**
	2	7.5	0.75	2.6	0	15.88	**No**	**No**	**No**
	3	8.5	0.82	2.51	0	15.73	**No**	**No**	**No**
	4	11.2	0.83	2.52	0	15.58	**No**	**No**	**No**
LG Fault	5	7	0.66	2.68	0.66	16.02	**No**	**No**	**No**
	6	7.5	0.75	2.6	0.75	15.88	**No**	**No**	**No**
	7	8.5	0.82	2.51	0.82	15.73	**No**	**No**	**No**
	8	11.2	0.83	2.52	0.83	15.58	**No**	**No**	**No**

4.2 Analysis in varying irradiation levels

This section peruses whether the NEC 2017 standards can reliably protect PV systems from LL/LG faults occurring in low irradiation levels. For which, two fault scenarios are analyzed for the same PV configuration as considered above: 1) Low mismatch impedance (7Ω) LL/LG fault cases in varying irradiation levels without MPPT and 2) Low mismatch impedance (7Ω) LL/LG fault cases in varying irradiation levels with MPPT.

4.2.1 LL and LG Fault analysis without MPPT

The variation in fault current magnitudes due to the changes in irradiation levels without MPPT is elucidated in Table 9. The statistics presented suggest that even for a low mismatch LL fault of 7Ω, the back fed OCPD current falls below the trip point of 7A to

5.61A once the irradiation level reaches 600W/m^2 (case 3 in Table 9). Moreover, the OCPD current further reduces significantly to 1.8A as the irradiation levels goes beyond 600W/m^2 to 200W/m^2 (see cases 3, 4 and 5). Therefore, even for low mismatch impedance faults, NEC 2017 standards are reliable to detect over currents only when the PV panels operate at an irradiance level above 600W/m^2. On the other hand, for LG faults, both OCPD and GFDI fuses are reliable up to an irradiation level of 800W/m^2 (case 6 and 7) while, OCPDs become insensitive in low irradiation levels and GFDI fuses alone protect the PV array in these conditions (case 8, 9 and 10). Note that the system configuration considered demands only 1A GFDI fuse. However, as discussed in previous sections, for higher rated systems that demands GFDI fuses up to 5A, LG faults occurring in low irradiation levels particularly below 400 W/m^2 will be hard to detect and isolate (case 9 and 10).

4.2.2 Impact of MPPT on LL and LG faults in varying irradiation levels

The effect of MPPT in similar aforesaid conditions has also been investigated and the outcomes are expressed in Table 10. As illustrated, for LL fault with MPPT, the OCPD current has drastically reduced to 2.68A from 9.38A even at an irradiance of 1000W/m^2 (case 1 in Table 10). As the irradiation further reduces from 1000W/m^2 to 200W/m^2, the MPPT operation further reduces the faulty string current from 2.68A to 0.43A (case 2 to 5). Similarly, in the analysis presented for LG faults (case 6 to case 10), the GFDI currents are 0.66A, 0.523A, 0.27A, 0.31A and 0.24A for 1000W/m^2, 800W/m^2, 600W/m^2, 400W/m^2 and 200W/m^2 respectively. For a better understanding, the change in operating points of the considered PV array with respect to fault, faulty string and array currents due to MPPT at various irradiation levels is depicted in Fig.6. As shown in Fig.6 (a), a notable difference in LG fault detection with respect to the previous analysis is that, the impact of MPPT is more severe in the case of LG faults. For instance, the reduction in GFDI current with MPPT at STC is as high as 12.07A (see Case 6 in Table 9 and case 6 in Table 10).

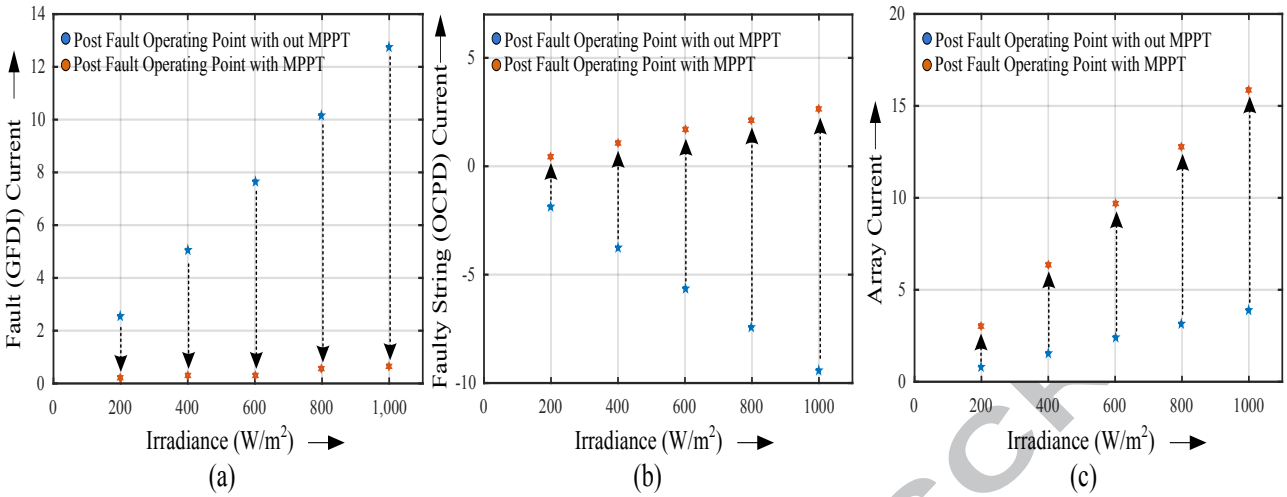

Fig.6. Effect of MPPT during LL/LG faults in varying irradiation levels: (a) Fault current, (b) Faulty string current and (c) Array current.

Table 9
LL and LG Fault analysis in varying irradiation levels without MPPT

Fault Type	Case No.	Irradiance (W/m^2)	Fault Current (A)	Faulty string OCPD current (A)	GFDI current (A)	Array Current (A)	OCPD Trip	GFDI Trip	Reliable Fault Detection
LL Fault with mismatch impedance of 7 ohms	1	1000	12.73	-9.38	0	3.95	Yes	**No**	Yes
	2	800	10.15	-7.47	0	3.173	Yes	**No**	Yes
	3	600	7.82	-5.61	0	2.35	**No**	**No**	**No**
	4	400	5.08	-3.74	0	1.545	**No**	**No**	**No**
	5	200	2.53	-1.86	0	0.75	**No**	**No**	**No**
LG Fault with mismatch impedance of 7 ohms	6	1000	12.73	-9.38	12.73	3.95	Yes	Yes	Yes
	7	800	10.15	-7.47	10.15	3.173	Yes	Yes	Yes
	8	600	7.82	-5.61	7.82	2.35	**No**	Yes	Yes
	9	400	5.08	-3.74	5.08	1.545	**No**	Yes	**No**
	10	200	2.53	-1.86	2.53	0.75	**No**	Yes	**No**

Table 10
LL and LG Fault analysis in varying irradiation levels with MPPT

Fault Type	Case No.	Irradiance (W/m^2)	Fault Current (A)	Faulty string OCPD current (A)	GFDI current (A)	Array Current (A)	OCPD Trip	GFDI Trip	Reliable Fault Detection
LL Fault with a fault impedance of 7 ohms	1	1000	0.66	2.68	0	15.88	**No**	**No**	**No**
	2	800	0.523	2.15	0	12.815	**No**	**No**	**No**
	3	600	0.27	1.74	0	9.72	**No**	**No**	**No**
	4	400	0.31	1.03	0	6.33	**No**	**No**	**No**
	5	200	0.24	0.43	0	3.05	**No**	**No**	**No**
LG Fault with a fault impedance of 7 ohms	6	1000	0.66	2.68	0.66	15.88	**No**	**No**	**No**
	7	800	0.523	2.15	0.523	12.815	**No**	**No**	**No**
	8	600	0.27	1.74	0.27	9.72	**No**	**No**	**No**
	9	400	0.31	1.03	0.31	6.33	**No**	**No**	**No**
	10	200	0.24	0.43	0.24	3.05	**No**	**No**	**No**

4.3 Generalizing the impact of LL and LG faults on the performance parameters in PV systems with/without MPPT

To generalize the MPPT effect, it is authoritative to study the impact of LL/LG faults in the system parameters for different PV configurations. To comprehend, two PV systems of different array sizes are considered for investigation: 1) Symmetrical 5×5 PV array and 2) Unsymmetrical 5×3 PV array. Both the arrays are built using the same PV module used for the experimentations in the previous section. To apprehend the overall behavior of a PV system in the presence of a fault, the fault current (GFDI current), faulty string current (OCPD current) and the total array current are analyzed for different LL and LG fault cases with varying mismatch levels with/without MPPT. Different mismatch impedances corresponding to different fault locations that have been taken into account vary in the range 7Ω to 11.2Ω (considered for fault analysis previously) and 10Ω to 16Ω for 5×5 and 5×3 PV array respectively. Simulation results obtained for different cases are depicted in Fig. 7(a) – Fig. 7(f). From the results attained, the following conclusions can be arrived: 1) System behavior is similar to both LL and LG faults in the presence/absence of MPPT for all the cases considered, 2) Irrespective of the array size, the pattern of variation in fault current, faulty string current and array current under faulty conditions of PV arrays remains identical, 3) MPPT operation optimizes the system operating point in the event of LL/LG faults such that the fault current magnitudes lie within a very small range, 4) Without MPPT controller, the faulty string experiences a heavy back fed current in the opposite direction and the current value approaches zero when the mismatch impedance reaches its maximum and 5) In the presence of MPPT, there is no post fault reverse current flow through the faulty string and the change in array current, string current and fault current are very minimal after MPPT optimization. Note that (3) and (4) derived in the previous section is applicable in case of abovementioned points 4 and 5 respectively to calculate the fault current levels. Further, the analysis clearly conveys that the behavior of LL and LG faults and its impact on the output parameters are always identical irrespective of the PV system type and its configuration.

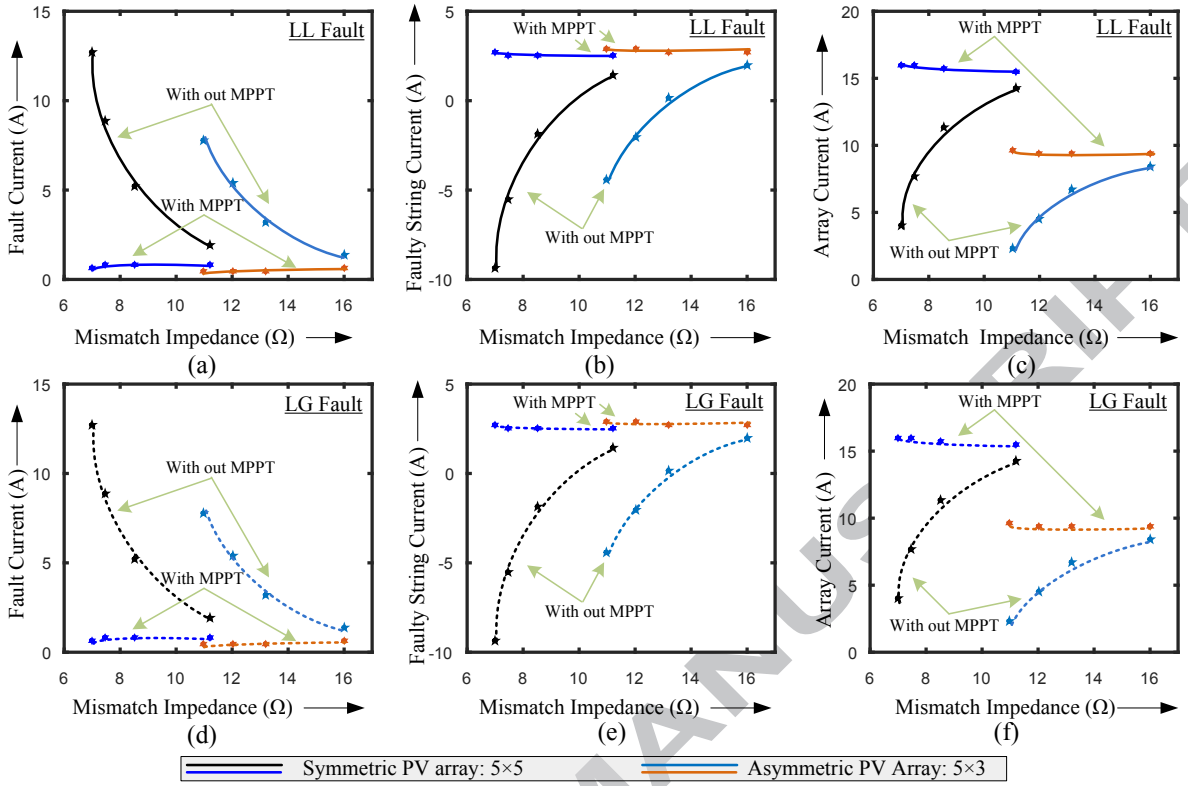

Fig.7. System behavior under faulty conditions with and without MPPT: (a-c) Fault current, Faulty string current and Array current in the case of LL faults and (d-f) Fault current, Faulty string current and Array current in the case of LG faults.

5. Experimental Validation and Discussions

To validate the simulation results discussed in the previous sections, a small scale laboratory prototype has been established and tested. Since the challenges in LL and LG fault detection in PV systems are primarily influenced by fault mismatch levels and MPP tracking technology, extensive experimental evaluations have been carried out in this section with respect to different PV array sizes to exclusively demonstrate the practical limitations involved in LL/LG fault detection.

5.1 Experimental Setup

For real-time experimentation, two different PV arrays are built using CHROMA 62050H PV simulator: 1) Symmetrical 5×5 PV array and 2) Unsymmetrical 5×3 PV array. To emulate the fault characteristics, different I-V patterns for the previously defined fault cases are programmed into the PV simulator. The MPPT algorithm utilized is simple Perturb and Observe (P&O) and is integrated to single stage DC-DC boost converter with the design specifications mentioned in Table 11. For execution, the MPPT algorithm is coded using an ARDUINO UNO controller at a switching frequency of 10 kHz. The PV simulator is

connected to a resistive load of 100Ω via the boost converter. Further, the output ripple of the boost converter is carefully designed to guarantee safe operation. The hardware prototype developed for real time interfacing between the boost converter and the PV simulator is demonstrated in Fig. 8. Experimentations have been performed by deploying the following sequential steps: 1) Operational transition from a normal to a faulty condition is considered for each experiment, 2) The sampling interval given for duty cycle feedback is set to 150ms in order to ensure steady state operation, 3) P&O is initialized at a duty cycle of 0.2 for all cases and 4) PV output voltage, current and power is recorded using a Mixed Scale Oscilloscope (MSO) for discussions.

Table 11
DC-DC Boost converter design specifications

S. No	Parameter	Rating
1	Switching Frequency	10 kHz
2	Inductor	1.1mH
3	Capacitor	10μF, 600V
4	Load Resistance	100Ω

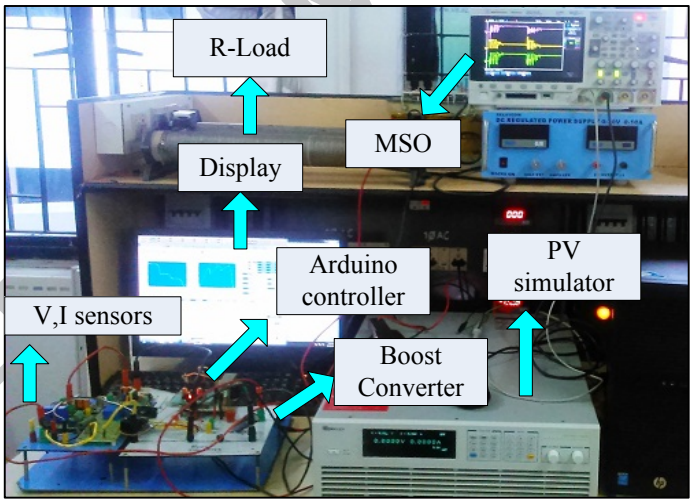

Fig.8. Hardware prototype developed for real time testing

5.2 Setting MPPT operating voltage range

Practically, MPPTs are integrated with the solar inverters itself. All grid tie/grid interactive inverters generally shut down if the open circuit voltage of the PV array (V_{oc}) falls below the start voltage of the inverter. Therefore, if post fault operating voltage of the PV array is less than the inverter start voltage, MPPTs normally do not function; and hence, the array operates at its open circuit conditions. This will allow the entire array current to flow through the fault points enabling the protection devices to trip. The inverter start voltage

is usually designed with respect to the MPPT operating range that is usually set to 30%-50% of the maximum voltage of the array. For confirmation, the data sheet specifications of various SMA inverters like SMA Sunny Boy 2000HFUS, 2500HFUS and 3000 HFUS are inspected and verified. Therefore, for the experiments conducted in this section, the minimum start voltage for the 5×5 and 5×3 PV arrays is designed for an MPPT operating voltage range between 36-100V. Now for the minimum MPPT operating voltage of 36V, the start voltage (open circuit voltage corresponding to 36V) is set as 45V.

5.3 Experiments on LL and LG Faults

As explained earlier, the impact of LL and LG faults on the output characteristics of the PV array are identical. Hence, LL and LG faults with same mismatch impedance are not separately considered for the hardware experiments. Further, the OCPD current and the GFDI current for a particular mismatch impedance can be easily calculated using Eq. (3), Eq. (4) and Eq. (6) derived in section 3. The transition of the 5×5 PV array from normal operation to 7Ω and 7.5Ω mismatch impedance faults without MPPT is shown in Fig. 9(a) and Fig. 9(b) respectively. GFDI current and OCPD current for these cases are calculated from the recorded array current using Eq. (6) and Eq. (3) respectively. For 7Ω fault, the GFDI and OCPD currents are 12A and 9A; while, at a lower mismatch level with mismatch impedance of 7.5 Ω, both the GFDI and OCPD currents significantly reduces to 8.5A and 5.4A respectively. As previously indicated via simulation in Table 7, OCPD rated at 7A according to NEC will not trip for the second case. Further, the effect of mismatch impedance is also evident and is exactly in line with the findings presented in Table 7.

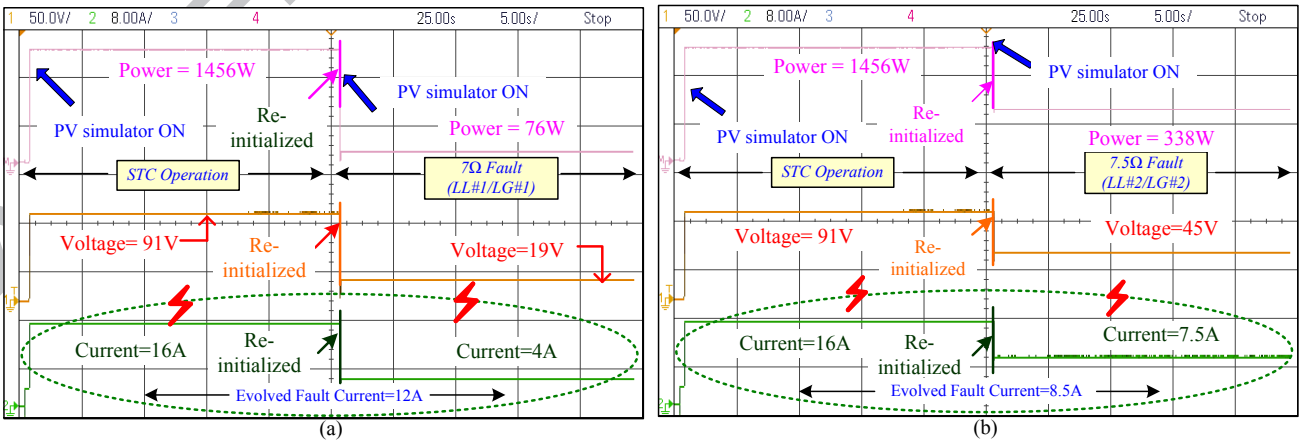

Fig.9. Experimental results for LL/LG faults at different mismatch impedances without MPPT: (a) 7Ω and (b) 7.5Ω

In order to evaluate the effect of MPPT in the fault current magnitudes, both 7Ω and 7.5Ω mismatch impedance faults are created in the presence of MPPT. The experimental

results are illustrated in Fig 10(a) and Fig 10(b) respectively. As shown in Fig. 10(a), for 7Ω fault, MPPT is non-operational as the post fault open circuit voltage (24V) falls below the minimum start voltage. Under such circumstances, the maximum fault current levels expressed in (6) and (7) flows through OCPD and GFDI fuses respectively; and thus trips the protection devices. However, in the case of LL/LG faults with 7.5Ω mismatch impedance faults, MPPT is operational and the post fault GFDI current is approximately optimized to 0A from 8.5A (non-MPPT case illustrated in Fig. 9). Further, as there is no reverse current flow, the OCPD current can be calculated using (4) and is approximately 3A; that is way below the trip point of 7A. To further enhance the understanding and to generalize the findings, the analysis based on MPPT is extended to a 5×3 PV array as well; having the same OCPD and GFDI trip points. Two faults of different mismatch impedances (previously explained in section 4.3) are evaluated: 1) 12Ω and 2) 13.5Ω. As shown in Fig. 11(a) and (b), for both faults, MPPT has optimized the magnitude of GFDI current to fall below the trip point of 1A. Also, the OCPD current for both cases calculated using is (4) is 3A. Overall, it can be concluded that MPPT optimization plays a crucial rule in reducing the fault current magnitudes and the present NEC recommendations are not suitable for PV systems with MPPT. It is important to note that, in the presence of MPPT, only LL/LG faults having high voltage mismatch can be detected.

6. Energy Loss and Income Analysis

Any undetected fault in a PV array will reduce the power output of the system. Hence, the considered 1.375 kW PV system has been tested to analyze the energy lost per annum, if a fault remains undetected in the PV array. The test results obtained are shown in Table 12. In normal operating conditions, the considered PV configuration can generate 3555.7 kWh of electricity considering 7 hours of peak sunshine per day. However, under faulty conditions, the units generated per annum significantly reduce and it can be clearly visualized in the statistics presented in Table 12. The impact of reduction in units generated can be gauged in terms of the income generation analysis. Under normal operation, the system generates an income of 711$ per year; that reduces up to 153$ in the case of an undetected LG/LL fault of impedance 7Ω characterized by a reduction of 2789.6W per year. Furthermore, even for a small PV configuration as considered here, the annual loss can go as high as 558$ that may further increase drastically in the case of PV power plants rated for large scale power generation. Consequently, the annual percentage energy losses due to undetected faults are 12.61%, 34.01%, 56.1% and 78.43% for 11.2Ω, 8.5Ω, 7.5Ω and 7Ω faults respectively. The

analysis clearly suggests the necessity of improving the present LL/LG fault detection standards.

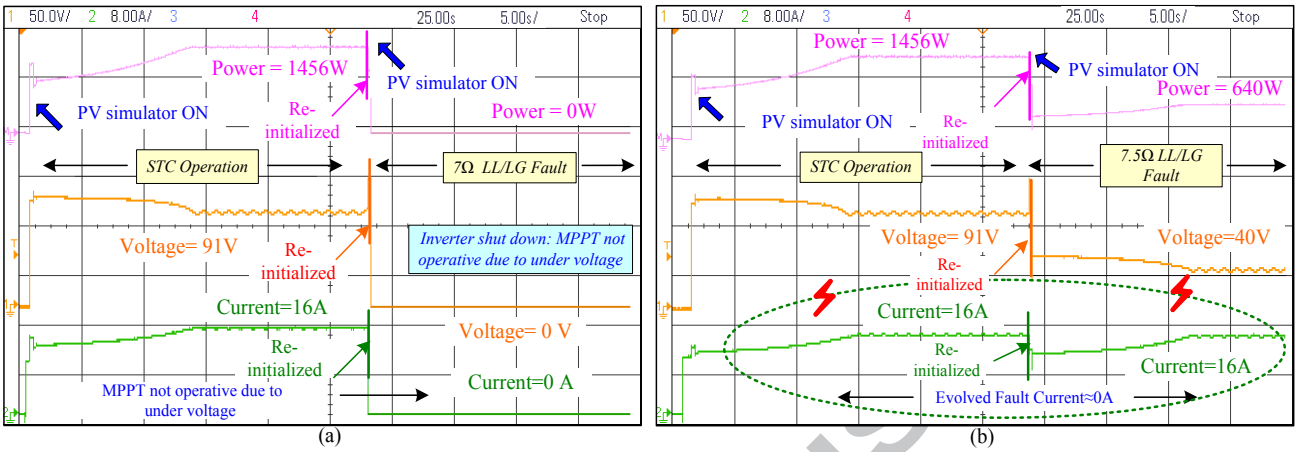

Fig.10. Experimental results for LL/LG faults at different mismatch impedances with MPPT: (a) 7Ω and (b) 7.5Ω

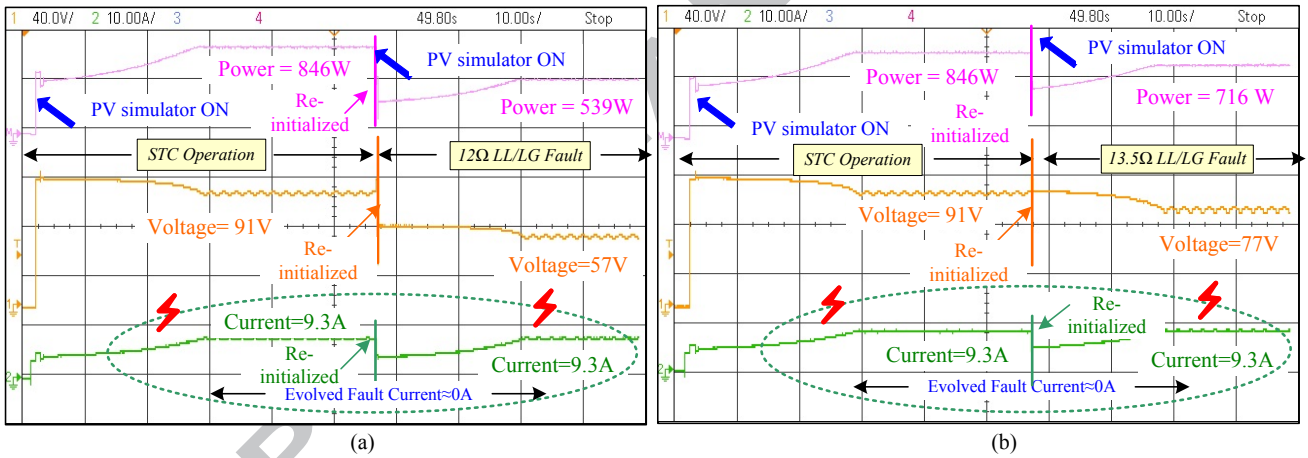

Fig.11. Experimental results for LL/LG faults at different mismatch impedances with MPPT in a 5×3 PV array: (a) 12Ω and (b) 13.5Ω

Table 12
Energy loss analysis due to undetected faults in a PV system

PV Status	Fault	Fault Impedance	Power output (W)	Energy generated per day (Wh)	Units generated per year (kWh)	Annual Income generated (.2$/unit)	Units lost due to undetected fault	Percentage Energy Loss	Annual Loss Incurred (.2$/unit)
Normal	-	-	1411	9877	3555.7	711$	-	-	-
Faulty	LL/LG	11.2	1233	8631	3107.1	622$	448.6	12.61%	89$
		8.5	931	6517	2346.1	470$	1209.6	34.01%	241$
		7.5	619	4333	1560	312$	1995.7	56.1%	399$
		7	304	2128	766.08	153$	2789.6	78.43%	558$

7. Suggestions to improve LL and LG fault detection in PV arrays

The protection standards defined in NEC 2017 focuses only to extend the applicability and flexibility of previous NEC standards. Besides, the conventional protection challenges

still exist in PV systems; particularly due to the inconsistencies in the selection of device ratings. The analysis carried out in this research points out the following challenges in the NEC standards: 1) OCPD standards are not sensitive enough to protect the PV array from high mismatch impedance LL faults, 2) Standards specified for the selection of GFDI fuse is not suitable to protect PV systems with higher power ratings, 3) With MPPT controller, proposed standards can neither detect LL nor LG faults in PV systems and 4) The standards formalized for the selection of OCPDs fails with changes in the instantaneous irradiation levels. Apart from these, non-availability of protection devices in the desired rating is also a major concern. Overall, the NEC 2017 standards: 1) Still cover only the universal fault scenarios in PV systems, 2) Lacks uniformity in varying operating conditions, 3) Not effective to provide sequential protection and 4) Fail to recommend supplementary protection standards that can avail reliable protection even if the primary standards fail. Overall, research advancements in the protection of PV systems needs immediate attention and still, there exists a potential research gap to find the optimal type, rating and location of protection devices to achieve reliable protection in PV systems. Based on the critical analysis performed, the following suggestions are likely to enhance fault detection in PV systems.

7.1 Improving existing NEC standards

One solution to counteract LL/LG fault detection problem is redefining the existing NEC standards such that, the probability of fault detection can be increased. In this context, the following points receive immediate attention: 1) *Interrelating conductor current carrying capacity in NEC 690.8 (B) with OCPD selection*: This is a major drawback in NEC standards recommended until 2017 since, in the case of undetected faults large PV systems, the string current may exceed the minimum current carrying capacity (defined in NEC 690.8 (B)) of the string conductors. Therefore, a better alternative is to select OCPDs based on the rated MPP current of the PV string, 2) *GFDI Selection based on DC rating of the inverter*: As the simulation and experimental results attained indicate, GFDI fuse selection based on the DC rating of inverters is not effective for large PV systems with less number of strings. Hence, it seems that fuse selection based on array voltage can be a more reliable option and 3) *Practicing same standards for MPPT and non-MPPT based PV systems*: NEC standards need to be redefined and differentiated between PV systems with MPPT and without MPPT as the steady state fault characteristics are entirely different and unique for both the cases.

7.2 Detecting the change in array operating voltage

The present conventions applied for LL and LG fault detection are based on detecting the uncharacteristic fault current levels. However, fault current level is not a trustworthy parameter to identify faults in PV systems because these fault current magnitudes are heavily dependent on the instantaneous irradiation levels, type of system and fault mismatch levels. On the other hand, even an LL/LG fault with low mismatch brings about an instantaneous significant reduction in array voltage [24]. While, in uniform irradiation levels, partial shading conditions and varying temperature levels, instantaneous change in operating voltage of the array is not as substantial as in the case of an LL/LG fault. Thus, similar to [24], LL/LG fault detection by monitoring the change in voltage levels is expected to a good and reliable solution to counteract the existing detection challenges.

7.3 Checking insulation resistance to detect LG faults

Irrespective of the mismatch impedance and MPPT operation, ground faults in PV arrays are usually associated with drastic reduction in insulation resistance between the array and the ground. Though instantaneous detection is not possible, monitoring insulation resistance with respect to the ground terminals can reliably detect LG faults in PV arrays. It is important to mention that, grid tie inverters designed according to IEC 62109-2 presently adheres such protection aspects. However, IEC 62109-2 are currently applicable only for inverters designed for ungrounded PV systems. In order to extend the application of IEC 62109-2 to grounded PV systems, researches confined to define suitable threshold limits for array insulation resistance in grounded PV systems are necessary. Thus, continuous online monitoring of array insulation resistance can be a viable option for reliable LG fault detection in future PV systems.

7.4 Incorporating supplementary detection schemes with existing standards

To counteract the limitations of existing protection standards, it is always beneficial to have a supplementary fault detection technique in a PV system. To be specific, along with the existing standards, integrating advanced fault detection approaches [25, 26] to PV installations can improve the fault detection possibilities to a great extent. However, selecting a suitable advanced fault detection approach for practical implementation needs decisive valuation based on the following factors: 1) environmental impact, 2) procedural complexity, 3) components required, 4) integration complexity, 5) detection time and 6) effect of noise. In addition, the supplementary detection schemes deployed must be capable to detect LL and LG faults in all unique operating conditions of the PV array. In this regard, some new and

advanced techniques that have been recently conceptualized are presented in [27-30]. Furthermore, detailed investigations regarding the features and selection criterions required for advanced detection LL/LG fault detection approaches are exemplified in [26].

8. Conclusion

This paper has presented a fundamental analysis on Line-Line and Line-Ground faults in PV arrays. The basic fault behavior, its evolution and its impact on the output parameters have been investigated. In addition, as NEC standards proclaimed to be the best protection standards available for PV systems, the compatibility of latest NEC 2017 standards has been critically analyzed with respect to numerous LL and LG fault cases under different operating conditions. Further, the challenges posed by MPPT in reducing the magnitude of fault current levels have also been examined. The experimentations performed were also extended to two different system configurations to generalize the findings. Based on the research outcomes, it has been verified that the current NEC protection standards are not suitable for LL/LG fault protection in PV systems; especially at low fault mismatch levels, low irradiation levels and in the presence of MPPTs. Furthermore, from the implications arrived, some important suggestions for future improvements are also suggested.

References:

[1] D. S. Pillai and N. Rajasekar, "A comprehensive review on protection challenges and fault diagnosis in PV systems." *Renew. and Sust. Energy Rev.,* vol. 91, pp. 18-40, Aug. 2018.

[2] B. Brooks, "The bakersfield fire-A lesson in ground-fault protection," *Solar Pro. Mag.*, pp. 62-70, Feb. 2011.

[3] *Electrical Installations of Buildings—Part 7: Requirements for Special Installations or Locations—Section 712: Solar PV Power Supply Systems, IEC Standard 60364-7-712, 2002.*

[4] *Photovoltaic (PV) arrays - Design requirements, IEC Standard 62548, 2013.*

[5] *Guide for Terrestrial PV Power System Safety, IEEE Standard 1374, 1998.*

[6] *Article 690: Solar PV Systems, 2008 National Electrical Code, ANSI/NFPA-70, National Fire Protection Association, Inc. Quincy, MA, 2011.*

[7] *Connection of PV Installations to the LV Network, Spanish Royal Decree 1663/2000, Sep. 29, 2000.*

[8] *Protection against Electric Shock—Common Aspects for Installation and Equipment, IEC Standard 61140, 2016.*

[9] *Installations—Part, Low-Voltage Electrical. Part 4-41: Protection for Safety—Protection against Electric Shock. IEC 60364-4-41, 2017.*

[10] W. Wiesner, W. Vaaßen, and F. Vaßen, "Safety aspects for installation and operation of grid connected PV plants," In *Proc. IEEE EPSEC*, pp. 1463-1467, 1992.

[11] P. G. Vidal, G. Almonacid, P. J. Pérez and J. Aguilera, "Measures used to protect people exposed to a PV generator: 'Univer project'," *Progress in Photovoltaics: Research and* applications, vol. 9, no. 1, pp. 57-67, Jan 2001.

[12] T.S. Key and D. Menicucci, "Practical application of the National Electrical Code to photovoltaic system design," In *Proc. IEEE EPSEC*, pp. 1110-1115, 1988.

[13] J. C. Hernandez and P. G. Vidal, "Guidelines for protection against electric shock in PV generators," *IEEE Trans. Energy Conversion*, vol. 24, no. 1, pp. 274-282, Mar. 2009.

[14] M. K. Alam F. Khan J. Johnson and J. Flicker, "A comprehensive review of catastrophic faults in PV arrays, " Types detection and mitigation techniques," *IEEE J. Photovoltaics*., vol. 5, no. 3, pp. 982-997, May 2015.

[15] J. Flicker and J. Johnson, "Analysis of fuses for blind spot ground fault detection in photovoltaic power systems," *Sandia National Laboratories Report*, Jun. 2013.

[16] W. Bower and J. Wiles, "Investigation of ground-fault protection devices for photovoltaic power system applications," In *Proc. IEEE PVSC*, pp. 1378-1383, 2000.

[17] Y. Zhao J. de Palma J. Mosesian R. Lyons and B. Lehman, "Line-line fault analysis and protection challenges in solar photovoltaic arrays," *IEEE Trans. Ind. Electron*., vol. 60, no. 9, pp. 3784-3795, Sep. 2013.

[18] Y. Zhao, B. Lehman, J. F. de Palma, J. Mosesian, and R. Lyons, "Challenges of over current protection devices in photovoltaic arrays brought by maximum power point tracker," in *Proc. 37th IEEE PVSC*, Seattle, WA, 2011, pp. 2472–2477.

[19] S. V. Dhople, A. Davoudi, A. D. Domínguez-García and P. L. Chapman, "A unified approach to reliability assessment of multiphase DC–DC converters in photovoltaic energy conversion systems," *IEEE Trans. Power Electron.,* vol. 27, no. 2, pp. 739-751, Feb. 2012.

[20] Park S, Kwon M, Choi S. Reactive Power P&O Anti-Islanding Method for a Grid-Connected Inverter With Critical Load. IEEE Transactions on Power Electronics. 2019 Jan;34(1):204-12.

[21] J. P. Ram, H. Manghani, D. S. Pillai, T. S. Babu, M. Miyatake and N. Rajasekar, "Analysis on solar PV emulators: A review," *Renewable and Sustainable Energy Reviews,* vol. 81, pp. 149–160, Jan. 2018.

[22] D. S. Pillai, J. P. Ram, M. S. S. Nihanth, and N. Rajasekar, "A simple, sensorless and fixed reconfiguration scheme for maximum power enhancement in PV systems." *Energy Conversion and Management*., vol. 172, pp. 402-417, Sep 2018

[23] D. S. Pillai, N. Rajasekar, J. P. Ram and V. K. Chinnaiyan, "Design and testing of two phase array reconfiguration procedure for maximizing power in solar PV systems under partial shade conditions (PSC)." *Energy Conversion and Management*., vol. 178, pp. 92-110, Dec 2018.

[24] D. S. Pillai and N. Rajasekar, " An MPPT based Sensorless Line-Line and Line-Ground Fault Detection Technique for PV systems," *IEEE Trans. Power Electrononics*, Early Access Article, Nov. 2018.

[25] D. S. Pillai and N. Rajasekar, "Metaheuristic algorithms for PV parameter identification: A comprehensive review with an application to threshold setting for fault detection in PV systems," *Renewable and Sustainable Energy Reviews,* vol. 82, no. 3, pp. 3503–3525, Feb. 2018.

[26] D. S. Pillai, F. Blaabjerg and N. Rajasekar "A Comparative Evaluation of Advanced Fault Detection Approaches for PV Systems," *IEEE journal of photovoltaics*, Early Access Article, Jan. 2019.

[27] Harrou F, Taghezouit B, Sun Y. Robust and flexible strategy for fault detection in grid-connected photovoltaic systems. *Energy Conversion and Management*. 2019 Jan 15;180:1153-66.

[28] Chen Z, Han F, Wu L, Yu J, Cheng S, Lin P, Chen H. Random forest based intelligent fault diagnosis for PV arrays using array voltage and string currents. *Energy Conversion and Management*. 2018 Dec 15;178:250-64.

[29] Madeti SR, Singh SN. Modeling of pv system based on experimental data for fault detection using knn method. *Solar Energy*. 2018 Oct 1;173:139-51.

[30] Roy S, Alam MK, Khan F, Johnson J, Flicker J. An irradiance-independent, robust ground-fault detection scheme for PV arrays based on spread spectrum time-domain reflectometry (SSTDR). *IEEE Transactions on Power Electronics*. 2018 Aug;33(8):7046-57.

HIGHLIGHTS

- Extended behavioral analysis on electrical faults in PV arrays is presented.
- Updates to in National Electric Code 2017 article 690 are studied.
- Impact of Maximum Power Pointing Trackers on fault detection has been examined.
- Compatibility of National Electric Code for array fault detection is investigated.
- Suggestions for improving fault detection in PV arrays are also conveyed.

Conflict of Interest

The authors whose names are listed immediately below report the following details of affiliation or involvement in an organization or entity with a financial or non-financial interest in the subject matter or materials discussed in this manuscript. Further, the authors hereby declare that there is no conflict of interest and for verification the names of the authors are listed below.

S.No	Name of the author	University
1	Dhanup.S.Pillai	Vellore Institute of Technology-Vellore
2	J. Prasanth Ram	KPR Institute of Engineering and Technology-Coimbatore
3	N. Rajasekar*	Vellore Institute of Technology-Vellore
4	Apel Mahmud	School of Engineering, Faculty of Science Engineering & Built Environment, Deakin University.
5	Yongheng Yang	Aalborg University, Aalborg
6	Frede Blaabjerg	Aalborg University, Aalborg